Annual balance and seasonal variability of sea-air CO2 fluxes in the Patagonia Sea: Their relationship with fronts and chlorophyll distribution

Alejandro A. Bianchi, Diana Ruiz-Pino, Hernán G. Isbert Perlender, Ana P. Osiroff, Valeria Segura, Vivian Lutz, Moira Luz Clara, Carlos F. Balestrini, Alberto R. Piola

Annual balance and seasonal variability of sea-air CO_2 fluxes in the Patagonia Sea: Their relationship with fronts and chlorophyll distribution

Alejandro A. Bianchi,[1,2] Diana Ruiz Pino,[3] Hernán G. Isbert Perlender,[2] Ana P. Osiroff,[1] Valeria Segura,[4] Vivian Lutz,[4,5] Moira Luz Clara,[2] Carlos F. Balestrini,[1] and Alberto R. Piola[1,2,5]

Received 7 April 2008; revised 22 October 2008; accepted 13 January 2009; published 25 March 2009.

[1] Sea-air differences of CO_2 partial pressures (ΔpCO_2) and surface chlorophyll *a* (chl-*a*) concentration have been determined during 22 cruises in various seasons for 2000–2006 over the Patagonia Sea and shelf break. From spring to autumn, the nearshore waters act as a source of atmospheric CO_2, while the midshelf and slope are a CO_2 sink, leading to highly negative areal means of sea-air CO_2 flux and ΔpCO_2. The ΔpCO_2 and CO_2 flux in spring reach values of -67 μatm and -7×10^{-3} mol m^{-2} d^{-1}, respectively, and are close to equilibrium in winter. Sea-air ΔpCO_2 and chl-*a* over the shelf are negatively correlated, suggesting that photosynthesis is one of the main processes responsible for the large CO_2 sequestration. The annual areal mean ΔpCO_2 and sea-air CO_2 flux are -31 μatm and -3.7×10^{-3} mol m^{-2} d^{-1}, respectively, indicating that the Patagonia Sea is one of the strongest CO_2 sinks per unit area in the World Ocean.

Citation: Bianchi, A. A., D. R. Pino, H. G. I. Perlender, A. P. Osiroff, V. Segura, V. Lutz, M. L. Clara, C. F. Balestrini, and A. R. Piola (2009), Annual balance and seasonal variability of sea-air CO_2 fluxes in the Patagonia Sea: Their relationship with fronts and chlorophyll distribution, *J. Geophys. Res.*, *114*, C03018, doi:10.1029/2008JC004854.

1. Introduction

[2] Atmospheric CO_2 is an important greenhouse gas and therefore plays a key role in modulating the planetary climate. As human activities in the last 150 years have raised atmospheric CO_2 by 100 ppm and doubling of preindustrial concentration is projected during this century [*Watson and Orr*, 2003; *Solomon et al.*, 2007], a major effect on global climate is expected. However, atmospheric CO_2 concentration has increased at a rate of only about 50% of that which is expected from all industrial CO_2 emissions. The oceans are presumably a major sink for CO_2. Hence, improved estimates of net flux across the air–sea interface are crucial for understanding the fate of CO_2 emitted into the Earth's atmosphere [*Broecker and Peng*, 1982; *Tans et al.*, 1990; *Takahashi et al.*, 1997].

[3] Hereafter the sea-air ΔpCO_2 will be referred to as DP and the sea-air CO_2 flux as FCO_2. The magnitude and direction of annual FCO_2 is governed by DP, CO_2 solubility, and wind speed. Since the air surface pCO_2 varies globally only 2.5% around the mean, currently approximately 380 μatm (data available from http://www.cmdl.NOAA.gov/ccgg/trends), the ocean, through its spatial and seasonal variations, is the main FCO_2 regulator. In addition, terrestrial ecosystems contributions may have a large impact in some coastal margins [*Cai et al.*, 2003]. In particular, the South Atlantic Ocean between 14 and 50°S is believed to be a sink of about -0.3 to -0.6 PgC a^{-1} [*Takahashi et al.*, 2002], which represent 15–30% of the net oceanic CO_2 uptake (2 PgC a^{-1}) [*Sarmiento and Gruber*, 2002; *Quay et al.*, 2003; *Sarmiento and Gruber*, 2006].

[4] The ocean marginal zone is among the most biogeochemically active areas of the biosphere. It receives massive continental inputs of C, N, and P and exchanges large amounts of these elements with the atmosphere and the open oceans. Marginal zones represent important, albeit often neglected, links in the global carbon cycle [*Chen et al.*, 2004]. Several studies have suggested the significance of marginal seas in the global sea-air CO_2 exchange [*Tsunogai et al.*, 1999; *Frankignoulle and Borges*, 2001; *DeGrandpre et al.*, 2002; *Cai et al.*, 2003; *Thomas et al.*, 2004; *Hales et al.*, 2005; *Bianchi et al.*, 2005]. However, there is a great uncertainty in the marginal contribution to the global CO_2 flux due to the diverse physical mechanisms that control the marine ecosystems.

[5] The area covered by the Patagonia Sea is close to 10^6 km^2, one of the largest shelf areas in the World Ocean. The shelf broadens from north to south, ranging from 170 km

[1]Departamento Oceanografía Servicio de Hidrografía Naval, Buenos Aires, Argentina.
[2]Departamento de Ciencias de la Atmósfera y los Océanos, Facultad de Ciencias Exactas y Naturales, Universidad de Buenos Aires, Buenos Aires, Argentina.
[3]Expérimentation et Approches Numériques, Laboratoire d'Océanographie et du Climat, Université Pierre et Marie Curie, Paris, France.
[4]Instituto Nacional de Investigación y Desarrollo Pesquero, Mar del Plata, Argentina.
[5]Consejo Nacional de Investigaciones Científicas y Técnicas, Buenos Aires, Argentina.

0148-0227/09/2008JC004854

at 38°S to more than 800 km south of 50°S. The main sources of shelf water masses are the subantarctic flows from the northern Drake Passage, through the Cape Horn Current [*Hart*, 1946] between the coast and the Malvinas Islands, and the Malvinas Current flowing northward along the shelf eastern border. The freshwater sources of the Patagonia shelf are due to the small continental discharge and the low-salinity water outflowing from the Magellan Strait. Several studies provide a detailed description of the Patagonia water masses and their circulation [*Lusquiños and Valdés*, 1971; *Bianchi et al.*, 1982; *Guerrero and Piola*, 1997; *Piola and Rivas*, 1997; *Bianchi et al.*, 2005].

[6] The biological response to fronts at every trophic level involves the extreme sensitivity of the ocean ecosystem to vertical motion [*Margalef*, 1963, 1978; *Holligan*, 1981; *Olson*, 2002]. Thus, DP and FCO_2 around fronts may be associated with the response of phytoplankton to the frontal environment. Two kinds of ocean fronts have been identified in the Argentine shelf, on the basis of hydrographic observations and satellite imagery [*Carreto et al.*, 1986; *Glorioso*, 1987; *Martos and Piccolo*, 1988; *Carreto et al.*, 1995; *Saraceno et al.* 2004; *Bianchi et al.* 2005; *Romero et al.*, 2006]: the shelf break front, a transition between the Malvinas Current waters and shelf waters, and tidal fronts, that develop in the warm season between vertically homogeneous coastal waters and stratified mid shelf waters. Tidal amplitudes in the Patagonian shelf are among the highest in the world ocean [*Kantha et al.*, 1995], and the energetic tidal currents interact with the bottom topography and coastal indentations vertically mixing coastal waters. These fronts had been analyzed by means of hydrography [*Sabatini et al.*, 2004; *Bianchi et al.*, 2005] and satellite derived SST [*Bava et al.*, 2002]. Using an 11 year time series of SST satellite images, *Bava et al.* [2002] conclude that tidal fronts in the Patagonia shelf were evident from spring to autumn.

[7] Vertical stratification, that plays a key role in the CO_2 dynamics, varies seasonally in the Patagonia Sea. The thermocline, as in most of temperate marginal seas, has a pronounced seasonal cycle. At the Patagonia shelf, the thermocline develops in spring, is intensified in summer, decays in autumn and is completely destroyed in wintertime [*Piola and Rivas*, 1997; *Rivas and Piola*, 2002]. The lack of spring and winter data precluded estimating annual budgets of DP and FCO_2. Therefore, new ΔpCO_2 data taken in spring and winter for the first time allows us to estimate the sea-air annual balance of DP and FCO_2 in the Patagonia Sea. On the basis of data collected from January to May, *Bianchi et al.* [2005] estimated DP and FCO_2 and used historical hydrographic data to study the links between vertical stratification and FCO_2 horizontal distribution in the Patagonia Sea. In the present study we use pCO_2 and chlorophyll data collected on the period 2000–2006 covering all seasons.

2. Data and Methods

[8] In the frame of two Argentine-French cooperative programs, a Global Environmental Facility (GEF) supported project and the Programme de Cooperation avec l'Argentine pour l'étude de l'océan Atlantique Austral (ARGAU), the annual CO_2 budget in the Patagonia Sea is estimated in this work.

[9] Seven ARGAU cruises and 3 GEF cruises were carried out aboard the Icebreaker Almirante Irizar and aboard the *R/V* Puerto Deseado, respectively (Figure 1 and Table 1). In the Icebreaker, near-surface (9 m depth) temperature, salinity, fluorescence and sea and air pCO_2 data were collected during nineteen transects between 2000 and 2005. The draft of the Icebraker intake may cause some bias in the chlorophyll data. The *R/V* Puerto Deseado underway data were collected at 3.5 m depth on the GEF cruises. In addition, CTD stations were taken on the GEF cruises (Figure 1 and Table 1). Underway data were averaged at 10 min intervals. Sea surface dissolved O_2 was measured every 3 hours during the ARGAU cruises and also at every CTD station in the three GEF cruises. Surface temperature and salinity were obtained with high-accuracy sensors (Sea Bird Electronics 37SI) in all cruises. The air and seawater pCO_2, were measured using an infrared technique described by *Takahashi* [1961] and *Copin-Montégut* [1985], with a system developed at the Laboratoire de Biogéochemie et Chemie Marines (LBCM) at the Université Pierre et Marie Curie in Paris. The system components are a flow through equilibrator and an IR analyzer (SIEMENS, type Ultramat 5F). The analyzer was calibrated with 3 gas standards of 270.0, 361.0, and 489.9 ppm mole fraction of CO_2. Atmospheric pCO2 was sampled every 6 h from an intake installed close to the bow of both vessels. High-accuracy sensors placed on the equilibrator provided temperature data that allow correcting for temperature changes. Seawater pCO_2 was also corrected for atmospheric pressure, drift and moisture effects. Except in regions of very high variability, such as ocean fronts, the standard deviation of water pCO_2 at 10 min intervals was about 1 μatm, in agreement with the results of *Metzl et al.* [1995]. Because of a malfunctioning in the IR analyzer during the first 8 days of the GEF 1 cruise, pCO_2 was estimated from total CO_2 and alkalinity. The pCO_2 standard error using these estimates was less than 7%. Total CO_2 (CT) and alkalinity (AT) were measured by means of a system also developed at LBCM, consisting in a 120 ml titration cell with two electrodes (a combined Ag-AgCl pHG201–7 and another REF 201 as reference) that allows measuring the electric potential change during a stepwise injection of 5 ml of a titrant solution. The titrant solution consisted in 0.1N HCl with 35g/l of NaCl. During the titration process, a curve of 31 equivalence points was built, which allows obtaining AT and CT values following *Gran* [1952]. These values were calibrated using Dickson standards, from the Marine Physical Laboratory at Scripps Institution of Oceanography, San Diego, U.S.A. During the ARGAU transects, chlorophyll a (chl-*a*) was determined from 1.5 to 2 L samples from the same water intake feeding the pCO_2 system and filtered through GF/F filters. The filters were stored in the dark at −20°C, and their analysis was carried out 2–3 months after each cruise, after adding 8 ml of 90% acetone. The extracts were read in a Beckman DU 650 spectrophotometer. Calculations of pigment concentrations were done according to *Strickland and Parsons* [1972]. Though the preferred method of storage of filters for pigment analysis is liquid nitrogen (−196°C), no liquid nitrogen container was available during the ARGAU cruises. Nevertheless, according to the tests ran by SCOR working Group 78 [*Mantoura et al.*, 1997], the recovery of chl-*a*, measured by HPLC, after 60 days would be ∼85%; and part of the chl-*a* would be

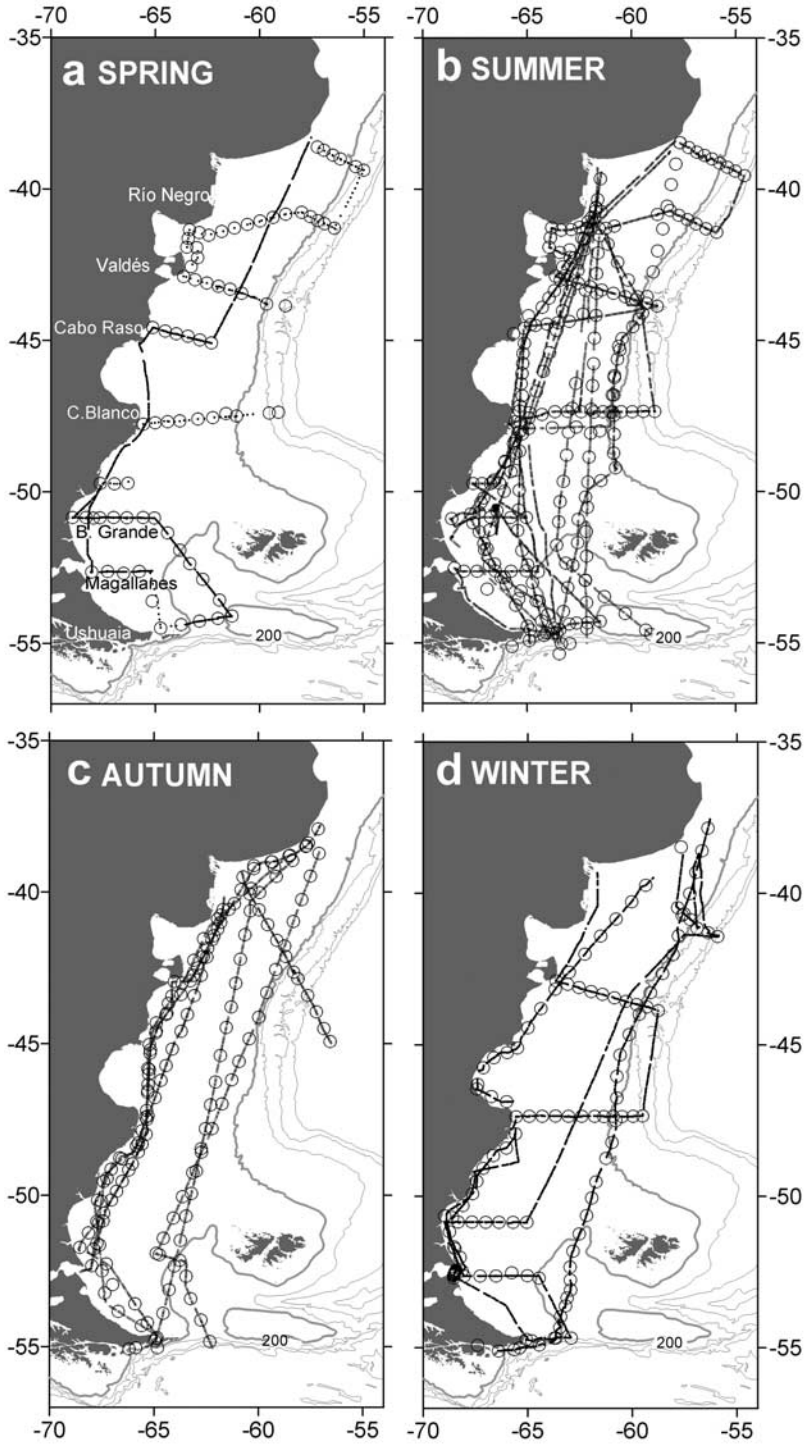

Figure 1. Location of ΔpCO_2 observations collected on icebreaker Almirante Irizar (ARGAU project) and Puerto Deseado (GEF cruises) for (a) spring, (b) summer, (c) autumn, and (d) winter. Large dots represent the sites for dissolved O_2 samples. The grey lines indicate the 200 (heavy), 1000, 2000, and 3000 m isobaths.

degraded to chlorophyllide-a and chlorophyll-a epimers and allomers. These degradation products (separated from chl-*a* by HPLC) would be read as if they were actual "chlorophyll-a" in the classic spectrophotometric method used for this set of samples, since their spectral characteristics cannot be distinguished. Hence, we expect that the recovery of chl-*a* was >85% in these samples.

[10] During the three GEF cruises, chl-*a* samples were collected with a surface bucket at each CTD station and underway at approximately 2 h intervals from a flow through system. Samples were filtered onto GF/F filters, and kept in liquid nitrogen (−196°C) on board and in ultra-freezer (−84°C) at the laboratory. The analysis followed the fluorometric method of *Holm-Hansen et al.* [1965]

Table 1. Details of the ARGAU Transects and GEF Cruises Used[a]

Cruise	Transect	Dates
ARGAU-0	0	24–25 March 2000
ARGAU-0	1	27–30 March 2000
ARGAU-0	3	11–12 May 2000
ARGAU-1	3	24–27 January 2001
ARGAU-1	4	19–21 February 2001
ARGAU-1	8	5–8 April 2001
ARGAU-1i	1	8–10 August 2001
ARGAU-1i	2	12–15 August 2001
ARGAU-2	1	31 January to 2 February 2002
ARGAU-2	6	23–27 March 2002
ARGAU-2	7	10–13 April 2002
ARGAU-2	10	3–5 May 2002
ARGAU-3	1	7–10 February 2003
ARGAU-3	10	15–18 May 2003
ARGAU-4	7	27 February to 1 March 2004
ARGAU-4	8	13–16 March 2004
ARGAU-4	11	14–18 April 2004
ARGAU-5	1	25–28 December 2004
ARGAU-5	9	9–12 April 2005
GEF 1	81[b]	9–28 October 2005
GEF 2	56[b]	10–30 March 2006
GEF 3	53[b]	7–25 September 2006

[a]The ARGAU data were collected on underway transects aboard Icebreaker Almirante Irizar.
[b]Occupied on GEF cruises from *R/V* Ara Puerto Deseado. Dissolved oxygen (and AOU) samples location are indicated by circles in Figure 1.

with some modifications [*Lutz et al.*, 2008]. Extracts were made in 100% methanol and read in a Perkin Elmer LS3 spectrofluorometer.

[11] Fluorescence was measured underway with a Turner model 2 fluorometer. The ratio between chl-*a* and in vivo fluorescence (*f*) varied between sample locations in all cruises. Therefore, to retrieve chl-*a* from the continuous in vivo fluorescence signal, *f* was calculated at two consecutive chl-*a* measurements and interpolated as a function of the distance at each intermediate point and then multiplied by fluorescence.

[12] Results obtained in the SOLAS Sea-Air Gas Exchange (SAGE) experiment clearly reveal a quadratic relation between wind speed and gas transfer velocity [*Ho et al.*, 2006] rather than a cubic relationship as proposed by *Wanninkhof and McGillis* [1999]. *Ho et al.* [2006] made a detailed comparison of the most commonly used wind speed/gas transfer relationships and the results of the SAGE experiment in the Western Pacific sector of the Southern Ocean. They proposed a new parameterization between wind speed and gas transfer velocity, consistent with coastal and open ocean estimates from previous studies at low wind speeds and SAGE results for higher wind speeds. Thus, the wind speed/gas transfer velocity (k_W) relationship proposed by *Ho et al.* [2006] is used in this study

$$kw = 0.266\left(\mathrm{Sc}(600)^{-1}\right)^{-1/2}\mathrm{U}_{10}^{2}, \quad (1)$$

where Sc is the Schmidt number, at in situ temperatures.

[13] To compute CO_2 fluxes, the effect of 3 variables must be taken into account: the CO_2 solubility in seawater (k_S), the coefficient of gas transfer velocity and ΔpCO_2. Then FCO_2 was estimated as follows:

$$\mathrm{FCO}_2 = k_S k_W \Delta p\mathrm{CO}_2. \quad (2)$$

[14] The CO_2 solubility was computed according to *Copin-Montégut* [1996]. It should be kept in mind that instantaneous wind data would capture weather extreme conditions not representative of the climate. In addition, the quadratic wind speed/gas transfer relationship used would enhance the weather influence in the FCO_2 calculations. Since the time scale for CO_2 exchange between the ocean mixed layer and the atmosphere is much longer (months) than wind speed variability. In the present work we use climatological monthly mean QuickScat wind speeds. The $0.25° \times 0.25°$ resolution wind speed data were monthly averaged during the 2000–2006 period and combined with in situ underway observations.

3. Results

3.1. Seasonal Variability of ΔpCO_2 and Chlorophyll *a* Distributions

[15] Figures 2 and 3 present the seasonally averaged surface distributions of DP and chl-*a* determined from all observations collected between late March 2000 and September 2006 (Table 1). Below these seasonal fields are described and analyzed in conjunction with selected hydrographic data.

3.1.1. Spring

[16] The spring DP and chl-*a* distributions are based on a single cruise carried out in October 2005 (Table 1). In this season, a broad part of the shelf and shelf break, from 39 to 50°S shows DP between −60 and −200 μatm covering more than 60% of the area (Figure 2a). The highest negative DP are observed at the shelf break between 40 and 43°S (less than −170 μatm) and offshore Cape Raso at the mid shelf (less than −150 μatm). South of 48°S the CO_2 sink is not as strong as in the northern region. In contrast, the CO_2 source regions are confined to San Matías Gulf (up to 30 μatm) and the nearshore areas of Peninsula Valdes (up to 35 μatm) and Grande Bay (less than 20 μatm). The areal mean DP in spring is −67 μatm and the associated FCO_2 is -7×10^{-3} mol m^{-2} d^{-1} (Figure 2a). In spring, regions of high chl-*a* (19 mg m^{-3}) are observed (Figure 3a) along the shelf break front, from 39 to 49°S. Inner and midshelf regions from 42 to 47°S also present high chl-*a* concentrations in a range from 1.5 to 6 mg m^{-3}. The highest chl-*a* concentrations in spring are estimated off Grande Bay (28 mg m^{-3}) were observed during GEF 1 cruise. There is a tight relation between the low DP and high chl-*a* (e.g., DP lower than −120 μatm off Grande Bay), suggesting a strong biological activity in austral spring (Figures 2a and 3a).

3.1.2. Summer

[17] The 25–28 December 2004 data (Table 1) were also analyzed as summer data. More than 80% of the region shows negative DP values and, consequently, negative FCO_2 (Figure 2b). Higher negative values of DP (as high as −95 μatm) are observed in the inner shelf, off Cape Raso and Peninsula Valdés. These regions are associated with relative chl-*a* maxima (≥3 mg m^{-3}). In the nearshore region from 39 to 43°S, there is a broad area of positive DP (≥80 μatm). This region is characterized by relatively high surface temperatures, especially in summer (>23°C [*Krepper and Bianchi*, 1982; *Guerrero and Piola*, 1997]), which increase pCO_2 in seawater. The higher temperature in the coastal area (4–5°C higher than the midshelf) would

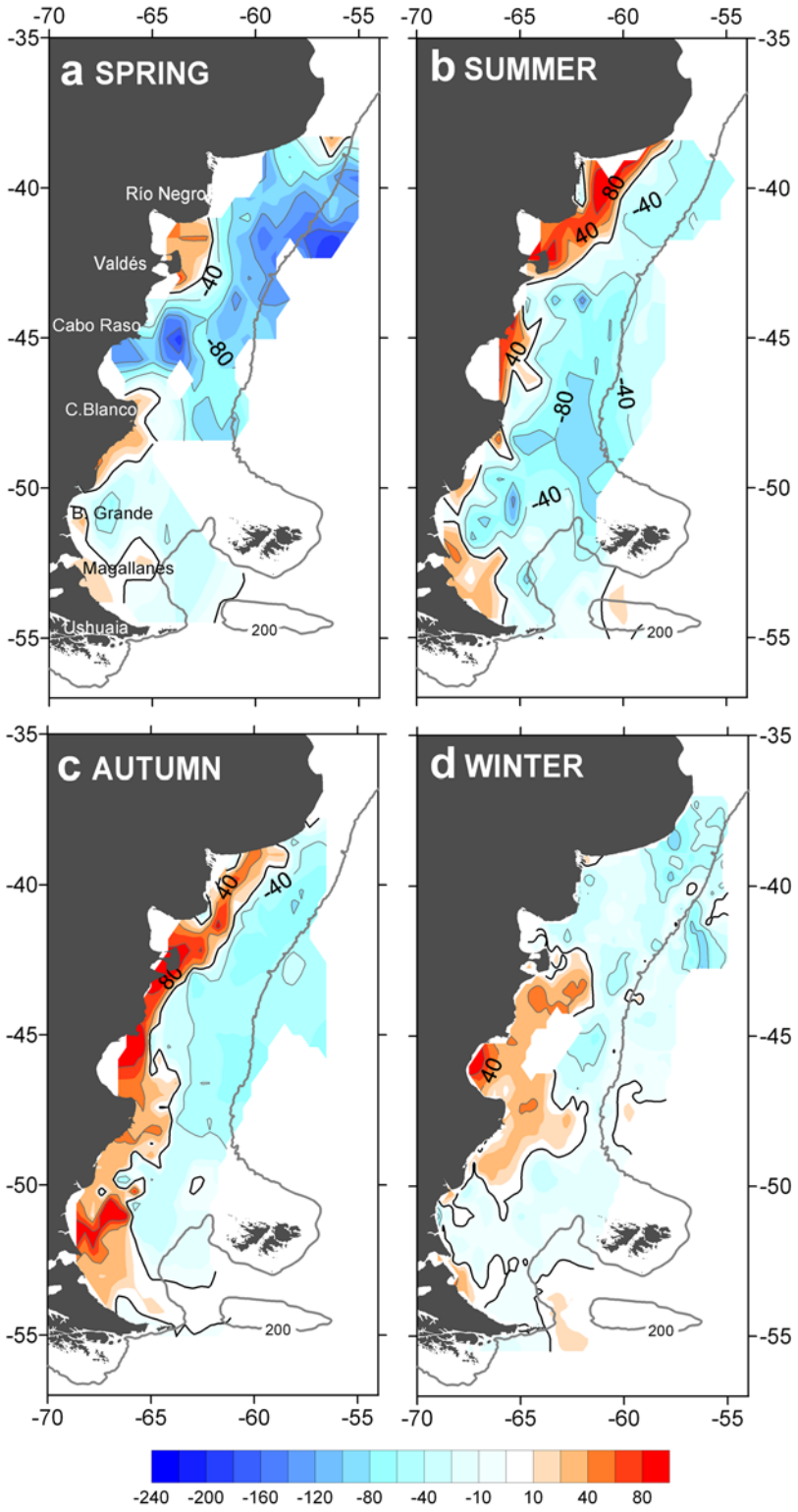

Figure 2. Horizontal distributions of sea-air ΔpCO_2, in μatm, collected in (a) spring, (b) summer, (c) autumn, and (d) winter. The heavy line is the 0 μatm contour. The 200 m isobath is shown.

increase the pCO_2 and reduce FCO_2 by about 20%. Since, the temperature difference does not fully explain the higher DP, differences in biological activity may be important in this region as well (see Discussion). The summer DP areal mean is -30 μatm and the associated FCO_2 is -3.8×10^{-3} mol m^{-2} d^{-1}. The highest chl-*a* values ($\geq$5 mg m^{-3}) are observed south of 51°S in the midshelf off Tierra del Fuego (Figure 3b). Other patches of high chl-*a* (>2 mg m^{-3}) are present off Peninsula Valdés, Cape Blanco and Grande Bay, all close to the location of main tidal fronts (Figure 4a). A DP decrease of 100 μatm is observed across the Valdés tidal front. This change is associated with a chl-*a* increase of

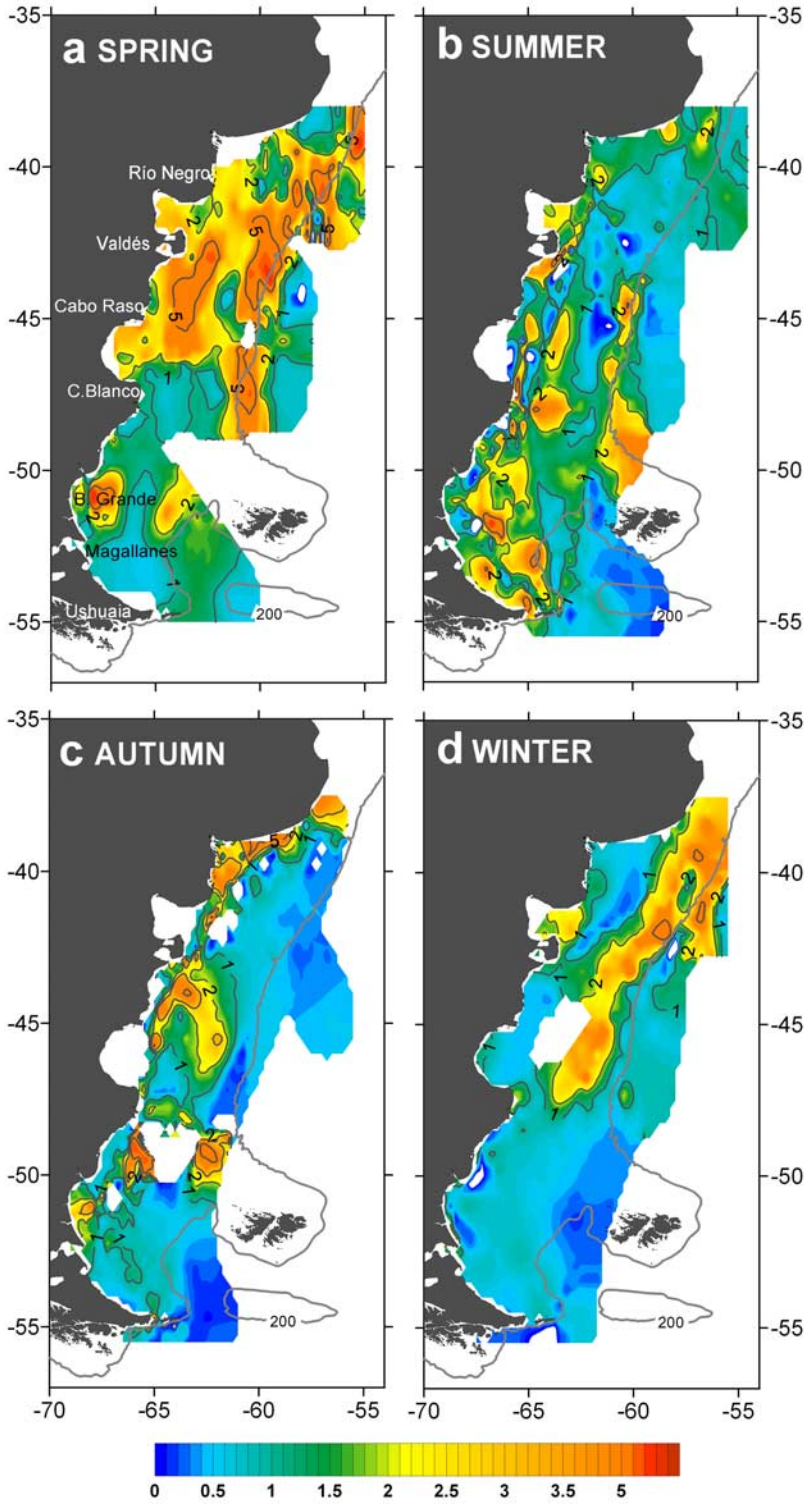

Figure 3. Surface chl-*a* distributions in (a) spring, (b) summer, (c) autumn, and (d) winter based on in situ observations. The 200 m isobath is shown.

2 mg m^{-3} (see Figure 2b and 3b). In contrast, in the Malvinas Current region, chl-*a* <1 mg m^{-3} is observed with increasing DP (see Figure 4c). The probable cause of this change in DP and relatively low chl-*a* is the decrease of stratification in the Malvinas waters (Figure 4b, see section 4).

3.1.3. Autumn

[18] The autumn data are from April and May; no data were collected in June (Table 1). The nearshore waters present positive DP over the whole study area while the stratified midshelf and outer shelf are CO_2 sinks (Figure 2c). The highest DP observed in this season exceeds 70 μatm at

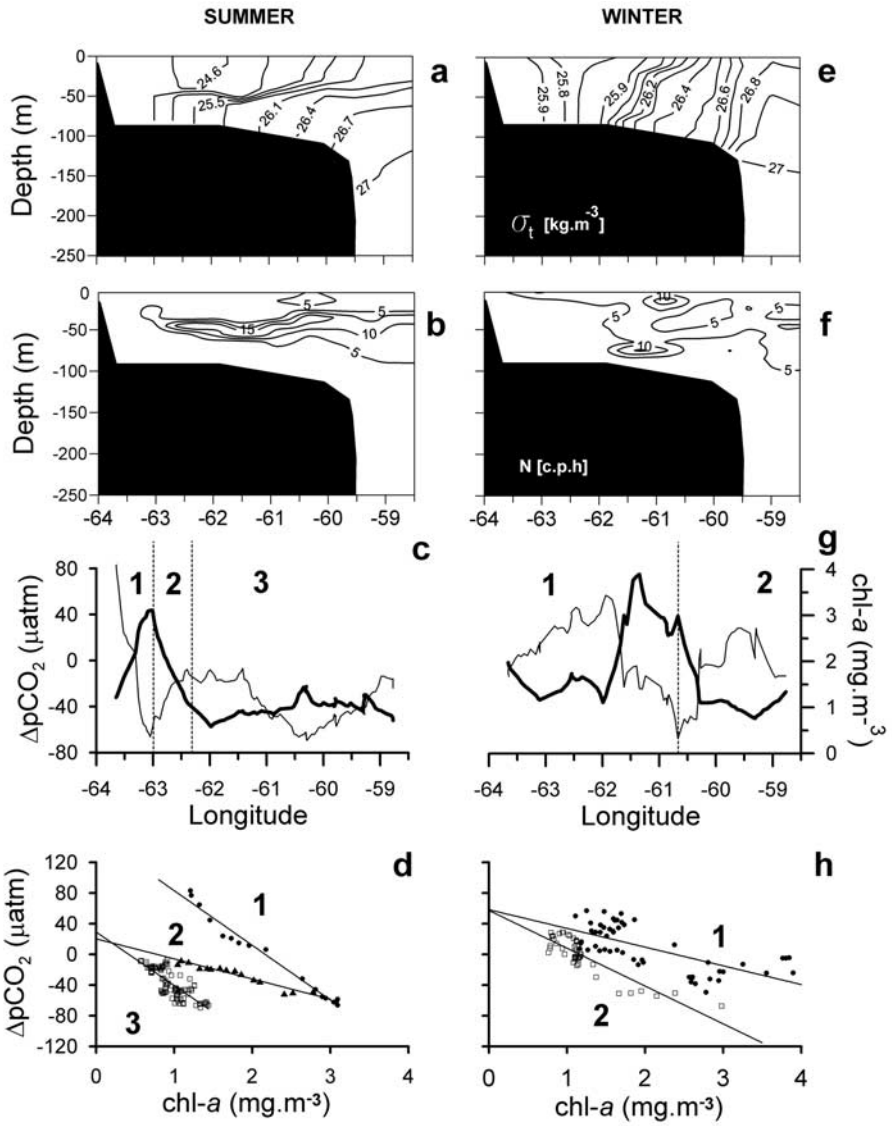

Figure 4. Summer and winter cross sections of (a and e) density (σ_θ, kg m^{-3}) and (b and f) Brunt-Väisälä frequency (cph) off Peninsula Valdés. (c and g) The surface chl-*a* (mg m^{-3}, bold line) and ΔpCO_2 (μatm, thin line) versus longitude. (d and h) Chl-*a* versus ΔpCO_2 linear regressions for different regimes indicated by the dashed lines in Figures 4c and 4g. In summer (Figure 4d) line 1 is from the coast to 63°W ($R^2 = 0.98$), line 2 is from 63°W to 62.4°W ($R^2 = 0.92$), and line 3 is for the remaining of the section ($R^2 = 0.62$). In winter (Figure 4h) line 1 is from the coast and 60.6°W ($R^2 = 0.48$) and line 2 is east of 60.6°W ($R^2 = 0.76$).

various near coastal locations and the lowest (−60 to −95 μatm) are found in most mid and outer shelves north of 47°S. The highest chl-*a* ($\geq$3 mg m^{-3}) are observed in the midshelf region at about 49−50°S and from 43 to 47°S, but DP-chl-*a* relation is not clear in this region. Note that the sampling is sparse in the midshelf region in autumn (Figure 1). The DP autumn areal mean is −20 μatm and the mean FCO_2 of -2.9×10^{-3} mol m^{-2} d^{-1}.

3.1.4. Winter

[19] The winter data are from August and September; no data were collected in July. Large amounts of heat lost to the atmosphere in fall and wind mixing, remove buoyancy from the upper layer leading to well-mixed water column in winter [*Rivas and Piola*, 2002]. The winter DP areal mean is slightly negative (−8 μatm) and associated with a mean FCO_2 of -1×10^{-3} mol m^{-2} d^{-1}. In winter, DP alternates from negative to positive regions (Figure 3d). The northeastern region (from 38 to 42°S) shows negative DP while in the inner shelf, from 43 to 49°S, a strong emission zone is observed, reaching 80 μatm at San Jorge Gulf. North of 45°S (Figure 2d), in the midshelf, relatively high values of chl-*a*, and high negative DP are observed, while in the inner shelf and shelf break areas DP is positive. In winter, the DP balance is close to equilibrium, though 70% of the region presents slight negative values. The areal mean chl-*a* (1.3 mg m^{-3}) is similar to summer and autumn values (Figure 3d).

Table 2. Seasonal and Annual Areal Mean Values of ΔpCO_2, Sea-Air CO_2 Flux and Chl-*a* in the Patagonia Sea[a]

	ΔpCO_2 (μatm)	Standard Error (μatm)	Sea-Air CO_2 Flux (10^{-3} mol m^{-2} d^{-1})	Chl-*a* (mg m^{-3})	Standard Error (mg m^{-3})	AOU (μmol kg^{-1})
Spring	−67	±4.0	−7	2.5	±0.12	−16
Summer	−30	±3.8	−3.8	1.4	±0.07	−11
Autumn	−20	±2.8	−2.9	1.2	±0.08	−7
Winter	−8	±1.7	−1	1.3	±0.07	−16
Annual	−31.3		−3.7	1.6		−12.5

[a]Standard errors are given for ΔpCO_2 and chl-*a*.

3.2. DP and Chl-*a* Relation in Peninsula de Valdés Leg

[20] DP and chl-*a* on a Peninsula de Valdés leg in summer present a tight correlation (Figure 4a–4d). From the coast to the tidal front (at 63°W), the water column is well mixed, while the vertical stratification is evident from the tidal front to the shelf break, close to 59°W (Figures 4a and 4b). Note that different chl-*a* versus ΔpCO_2 regressions (Figure 4d) result for the region west and east from the tidal front: line 1 from the coast to 63°W, where ΔpCO_2 decreased and chl-a increased (R^2 = 0.98); 2 from 63°W to 62.4°W, where ΔpCO_2 increased while chl-*a* decreased (R^2 = 0.92), and 3 east of 62.4°W, where the changes in ΔpCO_2 and chl-*a* are smoother (R^2 = 0.62).

[21] Since in winter the tidal front vanishes (Figures 4e–4g) we divided the section in two parts (Figure 4h): line 1 corresponds to the inner shelf region (from the coast to 60.6°W) where the correlation is lower (R^2 = 0.48). However, for the rest of the section (line 2), higher chl-*a* (see winter description above) east of 60.6°W is well correlated with negative values of DP (R^2 = 0.76).

3.3. Sea-Air CO_2 Fluxes: Annual Budget

[22] The areal averaged annual mean sea-air CO_2 flux based on the 2000–2006 data is -3.7×10^{-3} mol m^{-2} d^{-1} and the annual mean DP is −31.3 μatm. Thus, the Patagonia Sea acts as a strong sink of atmospheric CO_2 when compared to other marginal seas. On the basis of a more limited data set and a different wind speed/gas transfer velocity relationship, *Bianchi et al.* [2005] in a previous study, had estimated a very similar FCO_2 (about -4×10^{-3} mol m^{-2} d^{-1}) for the summer-autumn season only.

[23] Apparent Oxygen Utilization (AOU) areal means were estimated for the different seasons and all are negative (−9 to −16 μmol kg^{-1}), suggesting that near surface waters are supersaturated in response to photosynthetic activity. Seasonal areal mean values of DP, FCO_2, chl-*a* and AOU are given in Table 2. It can be seen, that DP and chl-*a* standard errors are 1 order of magnitude smaller than the seasonal means (Table 2).

4. Discussion

[24] On the basis of studies in the East China Sea, *Tsunogai et al.* [1999] proposed a "continental shelf pump" for the absorption of atmospheric CO_2 and subsequent exportation to the subsurface open ocean. If the world continental shelves would absorb atmospheric CO_2 at the rate observed in the East China Sea, this mechanism would account for a net CO_2 oceanic uptake of 1 PgC a^{-1}. Meanwhile, extrapolating the CO_2 uptake by the North Sea to all coastal seas, would produce a net CO_2 uptake of 0.4 PgC a^{-1} [*Thomas et al.*, 2004] which is about 20% of the global ocean's net annual uptake of anthropogenic CO_2 (1.9 ± 0.6 PgC a^{-1} [*Sarmiento and Gruber*, 2002]). It should be noted that *Sarmiento and Gruber* [2002] results are very similar to the estimates of anthropogenic CO_2 uptake by the ocean by *Bender et al.* [2005], using atmospheric O_2/N_2 (1.7 ± 0.5 PgC a^{-1}) and *Quay et al.* [2003], using changes in C^{13}/C^{12} (1.9 ± 0.4 PgC a^{-1}).

[25] Using satellite data to compute annual global net primary production and derived global particulate organic carbon, *Muller-Karger et al.* [2005], found that marginal seas may be responsible for at least 40% of the carbon sequestration in the ocean. Similar studies have been conducted in the South Atlantic Bight [*Cai et al.*, 2003] and the Middle Atlantic Bight [*DeGrandpre et al.*, 2002]. These areas albeit presenting some physical processes similar to the Patagonian Sea (seasonal stratification and CO_2 cycle) lead to significantly different results. *DeGrandpre et al.* [2002] found a net annual uptake of ~1×10^{-3} PgC a^{-1}, which is about 2 orders of magnitude smaller than other marginal seas. The reason for this difference is that new production appears to be counterbalanced by the increase in ocean pCO_2 due to summer heating and the pCO_2 never rises significantly above atmospheric saturation in these areas. Furthermore, the South Atlantic Bight, dominated by heterotrophic organisms, contrasts with the Patagonia Sea, acting as a source of CO_2 to the atmosphere while simultaneously exporting dissolved inorganic carbon (DIC) to the open ocean [*Cai et al.* 2003]. This sea-air CO_2 flux is opposite to the Patagonia Sea, probably because of different dominating marine ecosystems. The Patagonia Sea is dominated by autotrophic phytoplankton, mainly diatoms and dinoflagellates [*Lange*, 1985; *Schloss et al.*, 2007; *Almandoz et al.*, 2007].

[26] Different local studies have found that some continental shelves could act as sources of CO_2 [*Frankignoulle and Borges*, 2001; *Cai et al.*, 2003; *Borges et al.*, 2005]. Therefore, more field data are needed to constrain a world wide extrapolation. These large discrepancies show that the poor knowledge of the role of coastal ocean FCO_2 budget hampers an accurate quantification of the net ocean CO_2 absorption and the identification of missing CO_2 in the atmosphere.

[27] The observed atmospheric pCO_2 in the sampling periods reported here (Table 1) varied between 362 and 378 μatm. To evaluate the rate of time change of atmospheric pCO_2 over the region we estimated the mean atmospheric pCO_2 obtained during each ARGAU transect and during weekly periods for each GEF cruise. From 2000 to 2006, atmospheric pCO_2 presents a linear increase of 1.6 μatm a^{-1} (R^2 = 0.85). During this period the weekly mean atmospheric CO_2 observed at a coastal station in Ushuaia (data available

from http://www.cmdl.NOAA.gov/ccgg/trends) located at 55°S, near the southernmost tip of South America, also presents a positive trend (2.0 μatm a^{-1}), after correcting for the effects of water vapor and barometric pressure. The land station and marine atmospheric CO_2 trends are not significantly different at a 95% confidence level. The atmospheric pCO_2 trend estimated in Ushuaia is also virtually identical to the trend observed at Mauna Loa (data available from http://www.cmdl.NOAA.gov/ccgg/trends). Albeit the spatial and temporal sparseness of the marine sampling, the similarity between the land station and the shipborne derived trends, is indicative of the precision of our atmospheric CO_2 data measurements.

[28] The observations reveal that DP changes sign across ocean fronts, with positive (negative) values associated with well-mixed (stratified) waters. These DP changes across ocean fronts are in agreement with the results reported in our previous study [*Bianchi et al.*, 2005], on the basis of summer and fall observations collected prior to 2005. However, there is no apparent relation between the intensity of stratification and the magnitude of the CO_2 sink. For instance, weak stratification observed in spring leads to relatively high negative values of DP and high chl-*a* (not shown), which presumably reinforces the CO_2 oceanic uptake by photosynthetic processes.

[29] A zonal CO_2 section taken across the Patagonia Sea at approximately 47°S in December 1989 (data available at http://cdiac.esd.ornl.gov/oceans/pco2inv.html) shows an abrupt ocean pCO_2 decrease from 330 to 165 μatm at the shelf break (61°W). This observation is in good qualitative agreement with the results presented in this work. At this latitude our data across the shelf break, taken in late March 2006, the pCO_2 decrease is weaker, from 320 to 275 μatm, presumably because the pCO_2 from December are associated with the spring bloom, when a stronger uptake from the atmosphere is expected.

[30] The high pCO_2 observed in near coastal surface waters can be due to the upward flux of subsurface water with high CO_2 concentration as well as due to biological effects associated with inhibition of phytoplankton growth by the turbulent nature of the region and respiration of benthic and pelagic organisms. As the offshore upper layers are isopycnally connected to the inshore lower layers, they provide a possible pathway for tracer exchange across the tidal front and also a potential source of particulate and dissolved organic matter to the coastal region (Figure 4a). Similar DP variations across ocean fronts, associated with changes in stratification of northern and southern regions in the North Sea have been reported by *Thomas et al.* [2004]. Furthermore, *Hales et al.* [2005] reported that in summer most of the Oregon shelf was a CO_2 sink, while a vertically homogeneous nearshore strip was an intense source. Our observations also suggest the key role of stratification in the sea-air CO_2 balance.

[31] In summer, there is a strong DP decrease of about 150 μatm across the Valdés tidal front (Figure 4c). Note the high chl-*a* ($\sim$3 mg m^{-3}) and highly negative DP (-70 μatm) at the transition between well mixed ($N < 5$ cph, see Figure 4b) and stratified waters ($10 < N <$ and 20 cph), close to 63°W. Note also, the change in stratification across the tidal front and a much weaker transition between stratified and mixed waters in winter (see also regression lines in Figure 4d). At the shelf break front, located about 60°W, DP decreases to values observed at the tidal front ($<-70 \times 10^{-3}$ mol m^{-2} d^{-1}, Figure 4c) while chl-*a* increases only to $\sim$1.5 mg m^{-3}. At the eastern end of the section, close to the Malvinas Current waters, DP is much higher (-15 μatm), but surface chl-*a* shows a moderate increase ($\sim$1.2 mg m^{-3}, Figure 4c).

[32] The negative DP observed in winter (Figure 2d) in the northeastern region (north of 44°S and east of 60°W) and in the midshelf is probably associated with the onset of stratification in September, at the end of the cold season. In winter, at the shelf break area, negative DPs are only observed north of 43°S (Figure 2d). The surface layer heating over the shelf and subsequent onset of vertical stratification develops from north to south because of the latitudinal variation of the incoming solar radiation. Therefore, south of 45°S, where the water column is still unstratified, large CO_2 emission regions are observed between the coast and the midshelf, with DP of about 80 μatm. Slight stratification (2 cph at 35 m, Figure 4f) is observed between 60°30′ and 59°30′W, between the midshelf and the outer shelf in the Valdés leg (Figure 4c). This feature is associated with a sharp chl-*a* increase. Consequently, there is a strong correlation between chl-*a* and DP east of 61°W (Figure 4g). The DP minimum (about -70×10^{-3} mol m^{-2} d^{-1}), appears to be associated with slight stratification, and the chl-*a* was relatively high ($\sim$3 mg m^{-3}). In addition, the absence of the tidal front and the lack of stratification ($0 < N <$ 5 cph, Figure 4f) west of 61°W (Figure 4g) lead to a weak correlation ($R^2 = 0.48$, Figure 4h).

[33] The data reveal that during spring to autumn, the midshelf region is a CO_2 sink averaging approximately -9×10^{-3} mol m^{-2} $d^{-1}$and the magnitude of the CO_2 sink reaches values about -20×10^{-3} mol m^{-2} d^{-1} at the chl-*a* maxima, suggesting a modulation of the CO_2 fluxes by biological activity. *Romero et al.* [2006] showed that though large interannual chl-*a* variations are observed, the bloom locations remain relatively stable. Our results from in situ observations confirm the chl-*a* maxima close to the fronts.

[34] On the basis of all available O_2 data from 2000 to 2006 (Table 1), we estimate an annual areal mean surface AOU of -12.5 μmol kg^{-1} over the Patagonia Sea. This estimate is in agreement with previous results based on a smaller set of observations collected in summer and autumn from 2002 to 2004 [*Schloss et al.*, 2007]. The highest negative AOU (-16 μmol kg^{-1}) are observed in spring and winter (Table 2). We propose that the mechanisms leading to super saturation are distinct. In spring, the elevated O_2 is associated with photosynthetic activity, while in winter enhanced ventilation is induced by stronger winds [e.g., *Palma et al.*, 2004] which effectively steer the upper layer.

[35] The mean annual DP of -31.3 μatm is significantly lower than values estimated at other ocean regions [*Sweeney et al.*, 2002]. This DP and the associated FCO_2 are very similar to those estimated by *Thomas et al.* [2004] for the North Sea, which is considered one of the most important shelf CO_2 sinks. The averaged DP given by *Sweeney et al.* [2002] for the Temperate South Atlantic, which includes the open ocean from 15 to 50°S, adjacent to but not including the Patagonia Sea, is only -3.1 μatm, 1 order of magnitude lower than our estimate. Since satellite derived chlorophyll

data shows a sharp decrease across the Patagonia shelf break [e.g., *Romero et al.*, 2006], we propose that the striking difference between these neighboring regions is due to the large primary productivity at the Patagonia shelf and its high photosynthesis. Using a satellite-based model, *Behrenfeld and Falkowski* [1997] estimated a primary productivity of >300 gC m^{-2} a^{-1} at the Patagonia Shelf. Similarly, *Longhurst et al.* [1995] estimated 474 gC m^{-2} a^{-1} for the same region. The relationship found between DP and surface chlorophyll strongly suggests the impact of photosynthesis on CO_2 uptake. The in situ chlorophyll values observed in our study followed some general trends described by composite multi-annual satellite estimations of chl-*a* distribution [*Romero et al.*, 2006]; suggesting that the in situ chl-*a* used in our analysis are representative of regional distribution and adequately reveal the seasonal variability.

5. Summary and Conclusions

[36] Analysis of underway sea surface and atmospheric partial pressure of CO_2 collected between 2000 and 2006 on the Patagonia continental shelf reveals sharp seasonal changes. In situ chl-*a*, reveals a tight (negative) correlation between ΔpCO_2 and chl-*a*, suggesting that phytoplankton growth is a major factor controlling the capacity of the shelf to uptake atmospheric CO_2.

[37] The cross-shelf structure of DP and chl-*a* confirm our earlier conclusions [*Bianchi et al.*, 2005] about the key role of tidal and shelf break fronts on CO_2 dynamics. Changes in cross-shore vertical stratification from well mixed, to intensely stratified, to weakly stratified (in the warm period) exert a strong impact on the phytoplankton biomass and the sign and magnitude of sea-air CO_2 fluxes. Nevertheless, the Patagonia Sea acts as a strong sink of atmospheric CO_2, with an areal averaged annual balance DP of -31 μatm.

[38] Further analysis involving in situ observations on the rate of primary production will improve our understanding of the link between photosynthesis and DP in this region. Knowledge of the subsurface CO_2 and alkalinity distributions will help our understanding of CO_2 exchanges between the shelf and the open sea, and between surface and deeper waters.

[39] **Acknowledgments.** We greatly appreciate the comments of Taro Takahashi and two anonymous reviewers for their criticism on an earlier draft of this manuscript. This research was supported by Global Environmental Facilities (GEF) in the frame of PNUD ARG/02/018-GEF BIRF N° 28385-AR, subproject B-B46, and by Servicio de Hidrografía Naval. Additional funding was provided by grant CRN2076 from the Inter-American Institute for Global Change Research, which is supported by the U. S. National Science Foundation (grant GEO-0452325). Additional support was provided by the ARGAU Project, Instituto Antártico Argentino, Institut National de Sciences de l'Univers, Processus Biogeochimiques dans l'Océan et Flux, Université Pierre et Marie Curie, and the program ECOS-SECyT (A99U02). Additional financial support was provided by Agencia Nacional de Promoción Científica y Tecnológica (PICT99-0706420). QuikScat winds are produced by Remote Sensing Systems (RSS) and are supported by NASA Ocean Vector Winds Science Team. We are greatly indebted to officers and the crews of the Icebreaker Almirante Irizar and *R/V* Puerto Deseado.

References

Almandoz, G. O., M. Ferrario, G. A. Ferreyra, I. R. Schloss, J. L. Esteves, and F. E. Paparazzo (2007), The genus Pseudo-nitzschia (Bacillariophyceae) in continental shelf waters of Argentina (southwestern Atlantic Ocean, 38–55°8 S), *Harmful Algae*, *6*, 93–103, doi:10.1016/j.hal.2006.07.003.

Bava, J., D. A. Gagliardini, A. I. Dogliotti, and C. A. Lasta (2002), Annual distribution and variability of remotely sensed sea surface temperature fronts I the southwestern Atlantic Ocean, paper presented at 29th International Symposium on Remote Sensing of the Environment, Com. Nac. de Activ. Espaciales, Buenos Aires.

Behrenfeld, M. J., and P. G. Falkowski (1997), A consumer's guide to phytoplankton primary productivity models, *Limnol. Oceanogr.*, *42*(7), 1479–1491.

Bender, M. L., D. T. Ho, M. B. Hendricks, R. Mika, M. O. Bazttle, P. P. Tans, T. J. Conway, B. Sturtevant, and N. Cassar (2005), Atmospheric O_2/N_2 change1993–2002: Implications for the partitioning of fossil fuel CO_2 sequestration, *Global Biogeochem. Cycles*, *19*, GB4017, doi:10.1029/2004GB002410.

Bianchi, A. A., M. Massonneau, and R. M. Olivera (1982), Análisis estadístico de las características T-S del sector austral de la plataforma continental argentina, *Acta Oceanogr. Argent.*, *3*(1), 93–118.

Bianchi, A., L. Bianucci, A. Piola, D. Ruiz Pino, I. Schloss, A. Poisson, and C. Balestrini (2005), Vertical stratification and sea-air CO_2 fluxes in the Patagonian shelf, *J. Geophys. Res.*, *110*, C07003, doi:10.1029/2004JC002488.

Borges, A. V., B. Delille, and M. Frankignoulle (2005), Budgeting sinks and sources of CO_2 in the coastal ocean: Diversity of ecosystems counts, *Geophys. Res. Lett.*, *32*, L14601, doi:10.1029/2005GL023053.

Broecker, W. S., and T.-H. Peng (1982), *Tracers in the Sea*, Eldigio, Palisades, N. Y.

Cai, W.-J., Z. A. Wang, and Y. Wang (2003), The role of marsh-dominated heterotrophic continental margins in transport of CO_2 between the atmosphere, the land-sea interface and the ocean, *Geophys. Res. Lett.*, *30*(16), 1849, doi:10.1029/2003GL017633.

Carreto, J. I., H. R. Benavides, R. M. Negri, and P. D. Glorioso (1986), Toxic red tide in the Argentine Sea: Phytoplankton distribution and survival of the toxic dinoflagellate Gonyaulax excavata in a frontal area, *J. Plankton Res.*, *8*, 15–28, doi:10.1093/plankt/8.1.15.

Carreto, J. I., V. A. Lutz, M. O. Carignan, A. D. Cucchi Coleoni, and S. G. De Marco (1995), Hydrography and chlorophyll a in a transect from the coast to the shelf break in the Argentinian Sea, *Cont. Shelf Res.*, *15*, 315–336, doi:10.1016/0278-4343(94)E0001-3.

Chen, A., A. Andreev, K. Kim, and M. Yamamoto (2004), Roles of continental shelves and marginal seas in the biogeochemical cycles of the north Pacific Ocean, *J. Oceanogr.*, *60*(1), 17–44, doi:10.1023/B:JOCE.0000038316.56018.d4.

Copin-Montégut, C. (1985), A method for the continuous determination of the partial pressure of carbon dioxide in the upper ocean, *Mar. Chem.*, *17*, 13–21, doi:10.1016/0304-4203(85)90033-7.

Copin-Montégut, G. (1996), *Chimie de l'Eau de Mer*, 319 pp., Inst. Océanogr. de Paris, Paris.

DeGrandpre, M. D., G. J. Olbua, C. M. Beatty, and T. R. Hammar (2002), Air–sea CO_2 fluxes on the US Middle Atlantic Bight, *Deep Sea Res. Part II*, *49*, 4355–4367, doi:10.1016/S0967-0645(02)00122-4.

Frankignoulle, M., and A. V. Borges (2001), European continental shelf as a significant sink for atmospheric carbon dioxide, *Global Biogeochem. Cycles*, *15*(3), 569–576, doi:10.1029/2000GB001307.

Glorioso, P. D. (1987), Temperature distribution related to shelf-sea fronts on the Patagonian Shelf, *Cont. Shelf Res.*, *7*, 27–34, doi:10.1016/0278-4343(87)90061-6.

Gran, G. (1952), Determination of the equivalence point in potentiometric titrations, Part II, *Analyst*, *77*, 661–671, doi:10.1039/an9527700661.

Guerrero, R. A., and A. R. Piola (1997), Masas de agua en la plataforma continental, in *El Mar Argentino y sus Recursos Pesqueros: Antecedentes Históricos de las Exploraciones en el Mar y las Características Ambientales*, vol. 1, edited by E. E. Boschi, pp. 107–118, Inst. Nac. de Invest. y Desarrollo Pesquero, Mar del Plata, Argentina.

Hales, B., T. Takahashi, and L. Bandstra (2005), Atmospheric CO_2 uptake by a coastal upwelling system, *Global Biogeochem. Cycles*, *19*, GB1009, doi:10.1029/2004GB002295.

Hart, T. J. (1946), Report on trawling survey of the Patagonian continental shelf, *Discovery Rep.*, *23*, 223–248.

Ho, D. T., C. S. Law, M. J. Smith, P. Schlosser, M. Harveyand, and P. Hill (2006), Measurements of sea-air gas exchange at high wind speeds in the Southern Ocean: Implications for global parametrizations, *Geophys. Res. Lett.*, *33*, L16611, doi:10.1029/2006GL026817.

Holligan, P. M. (1981), Biological implications of fronts on the northwest European continental shelf, *Phil Trans. R. Soc. Ser. A*, *302*, 547–562.

Holm-Hansen, O., C. J. Lorenzen, R. W. Holmes, and D. H. Strickland (1965), Fluorometric determination of chlorophyll, *J. Conseil*, *30*(1), 3–15.

Kantha, L. H., C. Tierney, J. W. Lopez, S. D. Desai, M. E. Parke, and L. Drexler (1995), Barotropic tides in the global ocean from a nonlinear tidal model assimilating altimetric tides: 2. Altimetric and geophysical

implications, *J. Geophys. Res.*, *100*, 25,309–25,317, doi:10.1029/95JC02577.

Krepper, C. M., and A. A. Bianchi (1982), Balance del Mar Epicontinental Argentino, *Acta Oceanogr. Argent.*, *3*(1), 119–133.

Lange, C. B. (1985), Spatial and seasonal variations of diatom assemblages off the Argentine coast (south western Atlantic), *Oceanol. Acta*, *8*, 361–369.

Longhurst, A., S. Sathyendranath, T. Platt, and C. Caverhill (1995), An estimate of global primary production in the ocean from satelliteradiometer data, *J. Plankton Res.*, *17*, 1245–1271, doi:10.1093/plankt/17.6.1245.

Lusquiños, A. J., and A. J. Valdés (1971), Aportes al conocimiento de las masas de agua del Atlántico Sudoccidental, 48 pp., Serv. Hidrogr. Naval, Buenos Aires.

Lutz, V. A., V. Segura, A. I. Dogliotti, D. A. Gagliardini, A. A. Bianchi, and C. F. Balestrini (2008), Variability in the distribution of chlorophyll-a and primary production in the Argentine Sea using field and satellite estimations, extended abstract presented at 19th Ocean Optics Conference, Oceanogr. Soc., Tuscany, Italy, 6–10 Oct.

Mantoura, R. F. C., S. W. Wright, S. W. Jeffrey, R. G. Barlow, and D. E. Cummings (1997), Filtration and storage of pigments from microalgae, in *Phytoplankton Pigments in Oceanography: Guidelines to Modern Methods*, *Monogr. Oceanogr. Methodol.*, vol. 10, edited by S. W. Jeffrey, R. F. C. Mantoura, and S. W. Wright, pp. 261–282, U. N. Educ. Sci. and Cult. Org., Paris.

Margalef, R. (1963), Algunas regularidades en la distribución a escala pequeña y media de las poblaciones marinas de fitoplancton y en sus características funcionales, *Invest. Pesq.*, *23*, 169–230.

Margalef, R. (1978), Life-forms of phytoplankton as survival alternatives in an unstable environment, *Oceanol. Acta*, *1*, 493–510.

Martos, P., and M. C. Piccolo (1988), Hidrography of the Argentine Continental Shelf between 38° and 42°S, *Cont. Shelf Res.*, *8*(9), 1043–1056, doi:10.1016/0278-4343(88)90038-6.

Metzl, N., A. Poisson, F. Louanchi, C. Brunet, B. Schauer, and B. Bres (1995), Spatio-temporal distributions of sea-air fluxes of CO_2 in the Indian and Antarctic oceans: A first step, *Tellus B*, *47*, 56–60.

Muller-Karger, F. E., R. Varela, R. Thunell, R. Luerssen, C. Hu, and J. J. Walsh (2005), The importance of continental margins in the global carbon cycle, *Geophys. Res. Lett.*, *32*, L01602, doi:10.1029/2004GL021346.

Olson, D. B. (2002), Biophysical dynamics of ocean fronts, in *The Sea*, vol. 12, edited by A. R. Robinson, chap. 5, pp. 187–218, John Wiley, New York.

Palma, E. D., R. P. Matano, and A. R. Piola (2004), A numerical study of the southwestern Atlantic shelf circulation: 1. Barotropic response to tidal and wind forcing, *J. Geophys. Res.*, *109*, C08014, doi:10.1029/2004JC002315.

Piola, A. R., and A. L. Rivas (1997), Corrientes en la Plataforma Continental, in *El Mar Argentino y sus Recursos Pesqueros: Antecedentes Históricos de las Exploraciones en el Mar y las Características Ambientales*, vol. 1, edited by E. E. Boschi, pp. 119–132, Inst. Nac. de Invest. y Desarrollo Pesquero, Mar del Plata, Argentina.

Quay, P., R. Sommerup, T. Westby, J. Sutsman, and A. McNichol (2003), Changes in the $^{13}C/^{12}C$ of dissolved inorganic carbon in the ocean as a tracer of anthropogenic CO_2 uptake, *Global Biogeochem. Cycles*, *17*(1), 1004, doi:10.1029/2001GB001817.

Rivas, A. L., and A. R. Piola (2002), Vertical stratification on the shelf off northern Patagonia, *Cont. Shelf Res.*, *22*, 1549–1558, doi:10.1016/S0278-4343(02)00011-0.

Romero, S. L., A. R. Piola, M. Charo, and C. Eiras García (2006), Chlorophyll-*a* variability off Patagonia based on SeaWiFS data, *J. Geophys. Res.*, *111*, C05021, doi:10.1029/2005JC003244.

Sabatini, M. E., R. Reta, and R. Matano (2004), Circulation and zooplankton biomass distribution over the southern Patagonian shelf during late summer, *Cont. Shelf Res.*, *24*, 1359–1373, doi:10.1016/j.csr.2004.03.014.

Saraceno, M., C. Provost, A. R. Piola, J. Bava, and A. Gagliardini (2004), Brazil Malvinas Frontal System as seen from 9 years of advanced very high resolution radiometer data, *J. Geophys. Res.*, *109*, C05027, doi:10.1029/2003JC002127.

Sarmiento, J. L., and N. Gruber (2002), Sinks for anthropogenic carbon, *Phys. Today*, *55*, 30–36, doi:10.1063/1.1510279.

Sarmiento, J. L., and N. Gruber (2006), Carbon cycle, CO_2, and climate, in *Ocean Biogeochemical Dynamics*, chap.10, pp. 392–457, Princeton Univ. Press, Princeton, N. J.

Schloss, I. R., G. A. Ferreyra, M. E. Ferrario, G. Almandoz, R. Codina, A. A. Bianchi, C. F. Balestrini, and A. Poisson (2007), Role of plankton communities in pCO_2 sea-air exchange in the southwestern Atlantic Ocean, *Mar. Ecol. Prog. Ser.*, *332*, 93–106, doi:10.3354/meps332093.

Solomon, S., et al. (2007), Technical summary, in *Climate Change 2007: The Physical Science Basis. Contribution of Working Group I to the Fourth Assessment Report of the Intergovernmental Panel on Climate Change*, edited by S. Solomon, pp. 19–91, Cambridge Univ. Press, Cambridge, U. K.

Strickland, J. D. H., and T. R. Parsons (1972), *A Practical Handbook of Seawater Analysis*, 2nd ed., 310 pp., Fish. Res. Board Can., Ottawa, Ont.

Sweeney, C., T. Takahashi, and A. Gnanadeskian (2002), Spatial and temporal variability of surface water pCO_2 and sampling strategies, in *A Large-Scale CO_2 Observing Plan: In Situ Oceans and Atmosphere*, edited by M. Bender, NOAA, Springfield, Va.

Takahashi, T. (1961), Carbon dioxide in the atmosphere and in Atlantic Ocean water, *J. Geophys. Res.*, *66*(2), 477–494, doi:10.1029/JZ066i002p00477.

Takahashi, T., R. A. Feeely, R. F. Weiss, R. H. Wanninkhof, D. W. Chipman, S. C. Sutherland, and T. Takahashi (1997), Global air-sea flux of CO_2: An estimate based on measurements of sea–air pCO_2 difference, *Proc. Natl. Acad. Sci. U. S. A.*, *94*, 8292–8299, doi:10.1073/pnas.94.16.8292.

Takahashi, T., et al. (2002), Global sea-air CO_2 flux based on climatological surface ocean pCO_2 and seasonal biological and temperature effects, *Deep Sea Res. Part II*, *49*, 1601–1622, doi:10.1016/S0967-0645(02)00003-6.

Tans, P. P., I. Y. Fung, and T. Takahashi (1990), Observational constrains on the global atmospheric CO_2 budget, *Science*, *247*, 1431–1438, doi:10.1126/science.247.4949.1431.

Thomas, H., Y. Bozec, K. Elkalay, and H. J. W. de Baar (2004), Enhanced open ocean storage of CO_2 from shelf sea pumping, *Science*, *304*, 1005–1008.

Tsunogai, S., S. Watanabe, and T. Sato (1999), Is there a "continental shelf pump" for the absorption of atmospheric CO_2?, *Tellus B*, *51*, 701–712.

Wanninkhof, R., and W. R. McGillis (1999), A cubic relationship between sea-air CO_2 exchange and wind speed, *Geophys. Res. Lett.*, *26*(13), 1889–1892, doi:10.1029/1999GL900363.

Watson, A. J., and J. C. Orr (2003), Carbon dioxide fluxes in the global ocean, in *Ocean Biogeochemistry: A JGOFS Synthesis*, edited by M. Fasham et al., pp. 123–141, Springer, New York.

C. F. Balestrini, A. A. Bianchi, A. P. Osiroff, and A. R. Piola, Departamento Oceanografía Servicio de Hidrografía Naval, Avenue Montes de Oca 2124, 1271 Buenos Aires, Argentina. (abianchi@hidro.gov.ar; apiola@hidro.gov.ar)

M. L. Clara and H. G. I. Perlender, Departamento de Ciencias de la Atmósfera y los Océanos, Facultad de Ciencias Exactas y Naturales, Universidad de Buenos Aires, C1428 EHA Buenos Aires, Argentina.

V. Lutz and V. Segura, Instituto Nacional de Investigación y Desarrollo Pesquero, Paseo Victoria Ocampo 1, Escollera Norte, B7602HSA Mar del Plata, Argentina.

D. R. Pino, Expérimentation et Approches Numériques, Laboratoire d'Océanographie et du Climat, Université Pierre et Marie Curie, F-75252 Paris, France.